

Short Communication

## Investigation of Influence of Rice Husk Ash and Corn Cob Ash as Mineral Concrete Admixtures on Chloride Migration Using Electrochemical Technique

Jie Wang<sup>1</sup>, Honglin Guo<sup>2</sup>, Runduo Ding<sup>3,\*</sup>, Yonggang Zhang<sup>3</sup>

<sup>1</sup> Ningxia Haiping Expressway Management Co., Ltd., Yinchuan, Ningxia 750000, China

<sup>2</sup> Jilin Provincial Expressway Group Co., Ltd, Changchun Jilin 130000, China

<sup>3</sup> China Highway (Beijing) Engineering Material Technology Co., Ltd. Beijing 100088, China

\*E-mail: [dingrunze09876@sina.com](mailto:dingrunze09876@sina.com)

Received: 20 September 2022 / Accepted: 8 November 2022 / Published: 30 November 2022

The EIS method was used in the current study to investigate the chloride ion migration depth of Portland cement blended with rice husk ash (RHA) or corn cob ash (CCA), which was based on quantitative analyses of EIS data and electrochemical parameters of the equivalent circuit model to describe the ingress of chloride ions into cementitious media and determination of migration depth. The SEM and compressive strength analyses were also used to investigate the depth of chloride migration in the blended cement. The results of EIS analyses showed that increasing the content of RHA and CCA decreased chloride ion migration in cementitious media, and based on the findings, EIS analyses could predict the depth of chloride ion penetration in cementitious environments with different mineral admixture replacements. Furthermore, adding 10% RHA and 30% CCA to concrete cement (RHA10+CCA30) improves resistance to chloride ion migration and corrosion while also increasing the compressive strength of concrete after four weeks of curing time. Because the synergetic effect of RHA and CCA in RHA10+CCA30 can fill in the gaps between cement particles and aggregates, SEM analyses of steel rebar incorporated into the RHA10+CCA30 sample revealed lower pitting corrosion and corrosion products compared to the control sample (PC0).

**Keywords:** Chloride Migration; Mineral Admixtures; Portland cement; Rice Husk Ash; Corn Cob Ash; Compressive Strength; Electrochemical Technique

### 1. INTRODUCTION

Reinforced concrete structures, which are a combination of traditional cement concrete and reinforcements, are one of the most common types of structures used around the world [1, 2]. The coupling of steel and concrete can improve the compressive strength of concrete and the tensile strength of steel while also allowing engineers to design composite structures with complex architectural geometries at reasonable costs to withstand a variety of loads [3, 4].

When it comes to concrete durability, the most immediate threat is chloride attack. It is responsible for nearly 40% of concrete structure failures [5, 6]. Chloride attack corrodes steel in the presence of oxygen and water, significantly reducing structural strength [7]. Because of the exposure of concrete to seawater, the use of salt to melt the ice, and the presence of chlorides in the substances placed for storage, chlorides can penetrate concrete through capillary absorption, hydrostatic pressure, and diffusion [8, 9]. Chloride ion ingress in concrete occurs through the pore system and can be influenced by chloride ions binding to hydration products [10]. The chloride ions attack and catalyze the corrosion process by attacking the passive layer. Chloride ions degrade the passive layer and pit the steel reinforcement [11, 12].

To assess the risk of corrosion, it is necessary to investigate the chloride migration behavior in the concrete cover and near the steel reinforcement [13]. Concrete protects the reinforcing steel from penetrating chlorides, which can cause steel depassivation and an increase in the risk of steel corrosion [14].

Pozzolanic materials, such as mineral admixtures, have been shown in studies to reduce the dispersal and permeability of destructive chloride ions and moisture at the border of steel concrete, while also promoting its mechanical properties and long-term durability [15, 16]. These mineral additives from industrial waste and agricultural waste products such as metakaolin [17], sewage sludge ash [18], fly ash [19], bagasse ash [20], palm oil fuel ash [21], microsilica [22], marble dust [23] and silica fume [24] as low cost and eco-friendly additive have been investigated for their ability to enhance the durability of concrete and decrease reinforcement corrosion [25].

Corn is one of the most widely planted crops in the world, and its importance to the food industry cannot be overstated [26]. A large volume of corn cobs is formed as agricultural waste during the processing of corn. CCA waste is produced in the boilers of the animal feed industry [27, 28]. Several studies have shown that using CCA as a pozzolan in cement production can meet the minimum requirement of combined  $\text{SiO}_2$  and  $\text{Al}_2\text{O}_3$  of more than 70%, which a good pozzolan for the manufacture of blended cement should meet while also improving the workability of cement concrete [29-31]. Rice husk ash (RHA) is an agricultural waste that is usually regarded as an environmental hazard. RHA is a pozzolanic material that can be blended with cement for manufacturing concrete [32, 33]. Its use can reduce the environmental impact of the cement industry, producing efficient concrete with improved properties like impermeability, workability, strength, and corrosion resistance of steel reinforcement [34, 35].

The EIS method was used in this study to investigate the chloride ion migration depth of cement blended with RHA and/or CCA, which was based on quantitative analyses of EIS data and electrochemical parameters of the equivalent circuit model to describe the ingress of chloride ions into cementitious media and determination of migration depth. The SEM and compressive strength analyses were also used to investigate the depth of chloride migration in the blended cement.

## 2. EXPERIMENTAL

In this research, Portland cement (PC), coarse aggregates, corn cob ash (CCA; peripheral rural area of Shenyang, China), rice husk ash (RHA; power plant of Jilin Province, China), and water were

used to make construction concrete. Table 1 shows the chemical composition and physical properties of PC, CCA, and RHA. RHA (10%) and CCA (10-30%) were used as mineral admixtures at various concentrations and dry blended with PC. Table 2 shows five mixtures that were created and prepared for this project. The water-to-cement ratio was kept constant in all mixtures at 0.45.

**Table 1.** Chemical composition and physical properties of used PC, CCA and RHA in this study

Properties	PC	RHA	CCA
CaO (%)	64.20	0.39	10.73
SiO <sub>2</sub> (%)	19.90	68.32	8.50
Al <sub>2</sub> O <sub>3</sub>	4.11	1.32	11.19
SO <sub>3</sub> (%)	3.97	0.61	1.89
Mg(OH) <sub>2</sub> (%)	1.28	0.21	—
Fe <sub>2</sub> O <sub>3</sub>	2.71	0.56	1.16
Na <sub>2</sub> O (%)	0.18	3.81	0.17
Mg <sub>2</sub> O	1.71	3.61	10.21
K <sub>2</sub> O	0.69	3.19	0.79
Surface area (m <sup>2</sup> /kg)	310	19000	7441
Specific gravity (kg/cm <sup>3</sup> )	3.01	1.98	1.15
Loss on ignition (%)	1.01	13.29	1.11

**Table 2.** Mixture designs in this study.

Sample name	PC(wt%)	RHA(wt%)	CCA(wt%)
PC0	100	0	0
RHA10	90	10	0
CCA10	90	0	10
RHA10+CCA10	80	10	10
RHA10+CCA20	70	10	20
RHA10+CCA30	60	10	30

All designed mixtures were cast in 20cm cylinder steel molds for electrochemical studies. For 24 hours, the demolded samples were kept in an airtight curing chamber at room temperature with a relative humidity of at least 96%. The chemical composition of steel rebar is shown in Table 3.

**Table 3.** Chemical compositions of steel rebar.

<b>C</b>	<b>P</b>	<b>S</b>	<b>Ni</b>	<b>Mn</b>	<b>Si</b>	<b>Cr</b>	<b>Fe</b>
0.18	0.04	0.02	0.10	0.51	0.27	0.15	residual

The chloride diffusion on Portland cement was investigated using an electrochemical impedance spectroscopy (EIS) technique that included a system with steel rebar as the working electrode incorporated into the concrete samples, graphite as the counter electrode, and a KCl saturated Ag/AgCl electrode as the reference electrode. Concrete mixture designs were transported in cylindrical molds. The EIS experiments were conducted in the frequency range of  $10^{-2}$  Hz to  $10^5$  Hz in a 3.5 wt% NaCl solution as an aggressive ion media over an exposure time of 4 weeks.

The data for analyzing the chloride migration depth were generated through the soaking test, in which the test samples were immersed in a 3.5wt% NaCl solution at regular intervals. For evaluation of the depth of chloride migration, the prisms were first split on a compression-testing machine, and then the freshly split surfaces were sprayed with a 0.10 N AgNO<sub>3</sub> ( $\geq 99.0\%$ , Sigma-Aldrich) solution. The chemical reaction between AgNO<sub>3</sub> and chloride and hydroxide ions can lead to difference products that are used in chloride penetration measurements [36, 37]. In hardened matrix, the chemical reaction between AgNO<sub>3</sub> and present free-chloride can produce white precipitates of AgCl, whereas at greater depths wherever free-chlorides are absent, the chemical reaction between AgNO<sub>3</sub> and hydroxides can produce brown precipitates of AgO. Consequently, the depth of chloride migration can be easily determined using the color boundary change. ASTM C10911 was used to test the compressive strength of the samples. Scanning electron microscopy (SEM) was used to examine the surface morphology sample.

### 3. RESULTS AND DISCUSSION

#### 3.1. Electrochemical analyses

The Nyquist plots of steel rebar incorporated into the different mixture designs of PC samples (PC0, RHA10, CCA10, RHA10+CCA10, RHA10+CCA20 and RHA10+CCA30) after 3 days exposed in 3.5wt% NaCl media at room temperature are shown in Fig. 1a. The comparison between the Nyquist plots of PC0 and RHA10 indicates that the diameter of the semicircle is increased after the addition of RHA10 in concrete. Because of the microcrystalline nucleus and microaggregate filling effect, and because of the pozzolanic properties of RHA, the hardened cement paste is denser [38, 39], so that the ions' migration through the solid/liquid interface is blocked [40, 41]. A partial replacement of mineral additives in cement can improve the concrete's properties due to the pozzolanic reaction between calcium hydroxide and reactive silica in RHA in an alkaline environment [42, 43]. As a result, the amount of hydroxyl in solution decreases, and RHA-containing concrete has lower electrical conductivity than PC0. As a result of the mineral additives, the radius of the Nyquist curve is

increased. It is observed that the same change in Nyquist plots occurs after addition of CCA to cement or concrete, and increasing the amount of CCA in the cementitious system leads to a greater increase in radius of the Nyquist plots, indicating a further decrease in electrical conductivity and electromigration. The migration of chloride ions in a cementitious binary system can be tracked using Nyquist curves. Chloride ion diffusion has an efficient effect on solid-liquid phase interface in cementitious systems [44]. As a result, the  $R_{ct}$  can be used to study the diffusion of chloride ions. The bode plots presented in Figure 1b also demonstrate that the migration time contributes to the rise of the modulus value  $|z|$ .

The equivalent circuit model for fitting EIS data is presented in Figure 2 which contains  $R_s$  as solution resistance, and  $Q_1$  and  $R_{ct1}$  that refer to capacitance and resistance of the concrete specimens, respectively.  $Q_2$  and  $R_{ct2}$  demonstrate the double-layer capacitance and the charge-transfer resistance of steel rebar, respectively [45]. The  $R_{ct1}$  as the resistance of ion migration ions into the cement matrix can demonstrate the resistance of the charge transfer reaction of the hydration electrons, which is inversely proportional to the number of hydrated electrons that can undergo the electrochemical reaction in the internal structure of the cement matrix [46-48]. Thus, the obtained  $R_{ct1}$  values in Table 4 can describe the chloride migration in concrete matrix [46, 49], indicating the  $R_{ct1}$  value of RHA10+CCA30 is larger than the samples, and has higher resistance to the ion migration of chloride ions into the cement matrix. Therefore, RHA10+CCA30 was selected for further electrochemical studies.

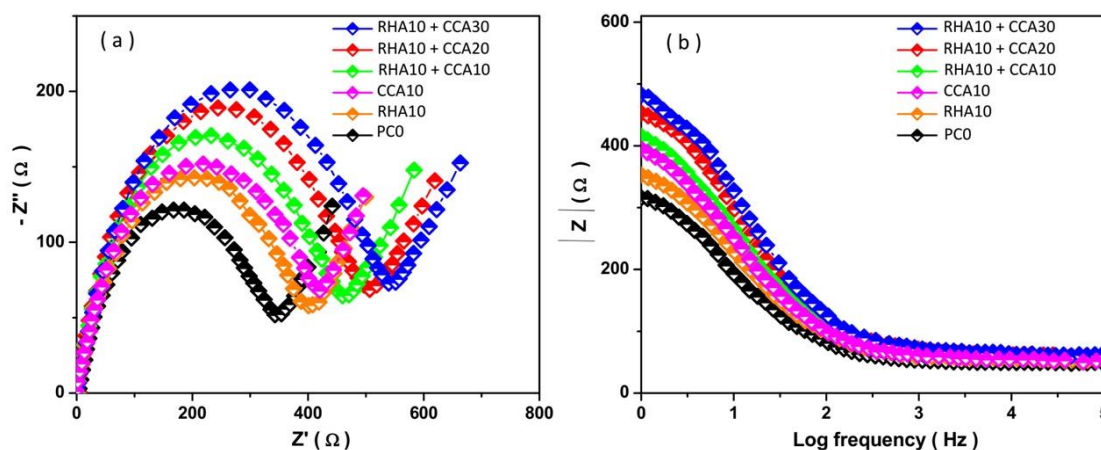


**Figure 1.** (a) Nyquist plots and (b) Bode plots of steel rebar incorporated into the different mixture designs of PC samples (PC0, RHA10, CCA10, RHA10+CCA10, RHA10+CCA20 and RHA10+CCA30) after 3 days exposure in 3.5wt% NaCl.

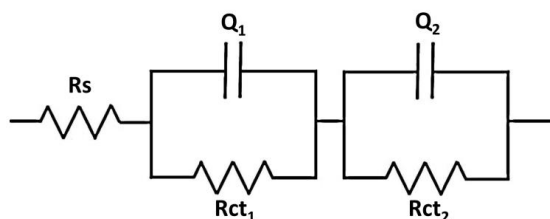


**Figure 2.** The equivalent circuit model for fitting EIS data.

Figure 3a depicts the Nyquist plots of steel rebar incorporated into the RHA10+CCA30 mixture design of a PC sample after different exposure times in 3.5wt% NaCl solution (0 day, 3 days, one week, two weeks, and four weeks). The Nyquist curves show that the migration of chloride ions reduces the diameter of semicircles, which is associated with an increase in the amount of chloride ions in the cementitious media [50, 51]. Figure 3b shows the bode plots, which show that the modulus-value increases as the migration time increases. The  $R_{ct1}$  values obtained from fitting the EIS data are shown in Table 4.

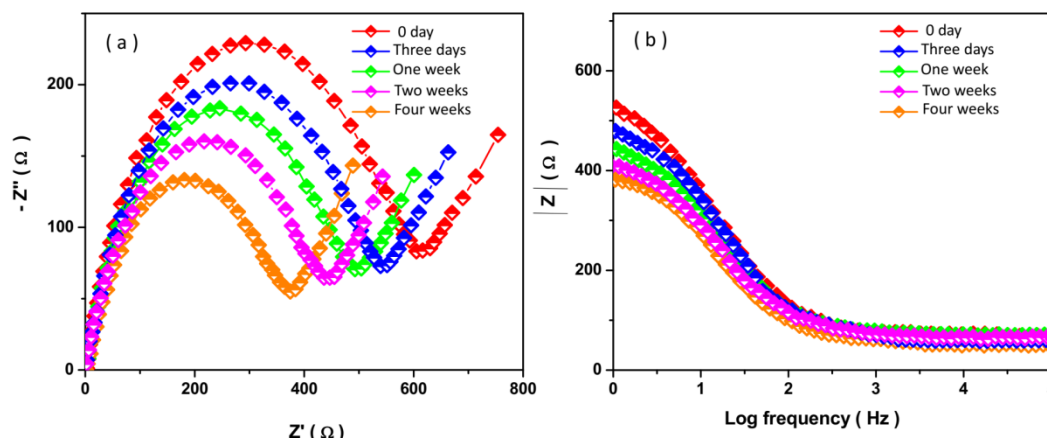


**Figure 3.** (a) Nyquist and (b) Bode plots of steel rebar incorporated into the RHA10+CCA30 mixture design of PC sample after different immersion time (0 day, 3 days, one week, two weeks and four weeks) in 3.5wt% NaCl solution at room temperature.

**Table 4.** The  $R_{ct1}$  values obtained from fitting the EIS data.

Mixture design	0 day ( $\Omega$ )	3 days ( $\Omega$ )	One week ( $\Omega$ )	Two weeks ( $\Omega$ )	Four weeks ( $\Omega$ )
PC0	455.5	367.2	310.1	201.9	35.5
RHA10	498.1	418.0	378.4	263.8	109.6
CCA10	522.4	453.1	415.4	317.0	150.1
RHA10+CCA10	546.8	488.0	452.5	370.3	190.7
RHA10+CCA20	594.5	545.8	510.3	443.3	260.7
RHA10+CCA30	621.9	593.5	540.7	471.7	341.1

With the increase in the migration time, the resistance of the ion transfer process  $R_{ct1}$  is decreased in the cementitious systems. The findings in Table 4 indicate that the following equation can describe the relationship between the  $R_{ct1}$  and chloride ion penetration depth (D) [52]:

$$D = (Rct_1(0) - Rct_1(t))^{0.5} \quad (1)$$

$Rct_1(0)$  and  $Rct_1(t)$  in this equation represent the values of  $Rct_1$  on the 0 day and after  $t$  days of migration, respectively. Figure 4 depicts the calculated chloride ion penetration depth. Based on the findings, it is clear that EIS analyses can predict the depth of chloride ion penetration in cementitious environments with different mineral admixture replacements.

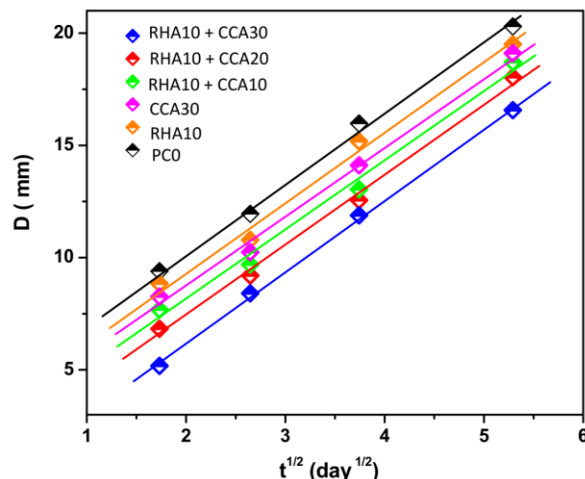


Figure 4. The calculated chloride ions penetration depth based equation  $D = (Rct_1(0) - Rct_1(t))^{0.5}$

### 3.2. Compressive strength analyses

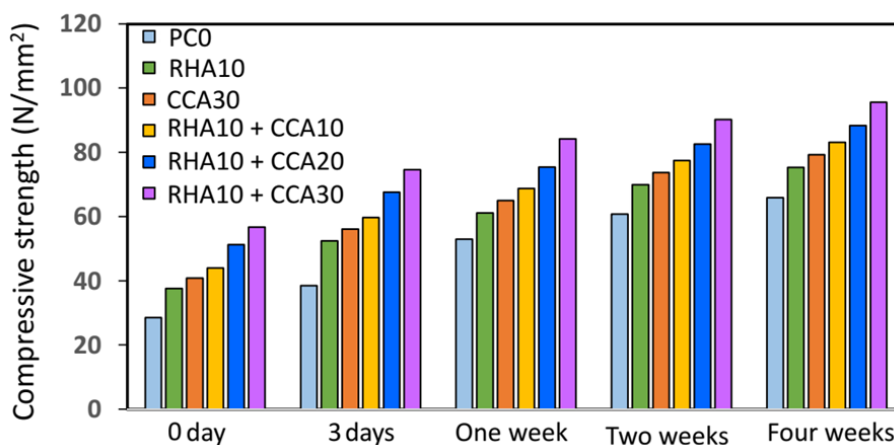
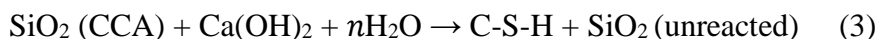


Figure 5. The compressive strength of the samples (PC0, RHA10, CCA10, RHA10+CCA10, RHA10+CCA20 and RHA10+CCA30) at different exposure period (0 day, 3 days, one week, two weeks and four weeks).

The compressive strengths of the samples (PC0, RHA10, CCA10, RHA10+CCA10, RHA10+CCA20 and RHA10+CCA30) at different exposure periods (0 day, 3 days, one week, two weeks and four weeks) are exhibited in Figure 5. The comparison between the compressive strengths of PC0 and RHA10 indicates that the addition of RHA to mixture design of PC samples promotes the

compressive strength because of the pozzolanic reaction and microfiller effect of the RHA [53]. The microfiller effect of RHA can effectively distribute the hydration products in a more homogeneous fashion in the available space, making the matrix much denser [53, 54]. Furthermore, it is observed that the RHA10+CCA30 mixture design of the PC sample shows the maximum compressive strength at long exposure periods compared to the other samples. It can be suggested that the higher compressive strength of RHA10+CCA30 can be related to the higher content of the sum of SiO<sub>2</sub>, Al<sub>2</sub>O<sub>3</sub> and Fe<sub>2</sub>O<sub>3</sub> in the chemical composition of CCA and its pozzolanic nature [55, 56]. The findings display that CCA blended cement concrete gains strength slowly at an early curing age. It was attributed to this fact that the pozzolanic reaction at room temperature is slow and, thereby, a longer curing period is needed to observe its positive effects which is in agreement with the results from previous studies [30, 55]. Moreover, with increasing the CCA content in mixture design of PC samples, the compressive strength is increased due to the formation of cement gel under pozzolanic reactions between the amorphous SiO<sub>2</sub> from CCA and water reactions to produce amorphous calcium silicate hydrate (termed as the C-S-H gel) and Ca(OH)<sub>2</sub> in paste [55]. The suggested mechanism of cement hydration with CCA is presented in the following equations (2) and (3) [55, 57].



Additionally, the higher content of Al<sub>2</sub>O<sub>3</sub> in CCA as a partial replacement by cement is due to lime-alumina-calcium sulfate (C-A-H) gel formation in concrete. Al<sub>2</sub>O<sub>3</sub> in amorphous or glassy forms is the major component of a pozzolan which can react with Ca(OH)<sub>2</sub> formed from the hydration of calcium aluminates [58]. The rate of the pozzolanic reactions is proportional to the content of Al<sub>2</sub>O<sub>3</sub> in mineral admixtures for reaction [59]. Therefore, the synergetic effect of RHA and CCA in RHA10+CCA30 can fill in the gaps between cement particles and aggregates and, as a result, decrease the friction between particles and enhance the workability and compressive strength of concrete. The lower specific gravity of CCA and RHA particles toward the cement particles also contributes to promoting the compressive strength of the RHA10+CCA30 concrete sample [60].

### 3.3. Morphological analyses

Figures 6a and 6b show SEM micrographs of carbon steel rebar in PC0 and RHA10+CCA30 concrete samples after two weeks of immersion in 3.5wt% NaCl solution. The comparison of the SEM micrographs of steel rebar in the PC0 and RHA10+CCA30 samples shows fewer pitting corrosion and lower corrosion products on the steel rebar surface incorporated into the RHA10+CCA30 sample, implying mild pitting corrosion due to a decrease in chloride ion permeation in aggressive reinforced concrete environments. The smaller diameter pore on the surface of the steel rebar incorporated into the RHA10+CCA30 sample also shows that large diameter pores have transformed to smaller pores due to the addition of RHA and CCA in cement of concrete which fill in the gaps between cement particles because of the filling effect of RHA and CCA before pozzolanic reaction starts [61]. Consequently, the pit cover effect hinders diffusion of corrosion products from the pit, which improves

the resistance to corrosion of steel rebar which is in agreement with the results from compressive strength and electrochemical analyses.

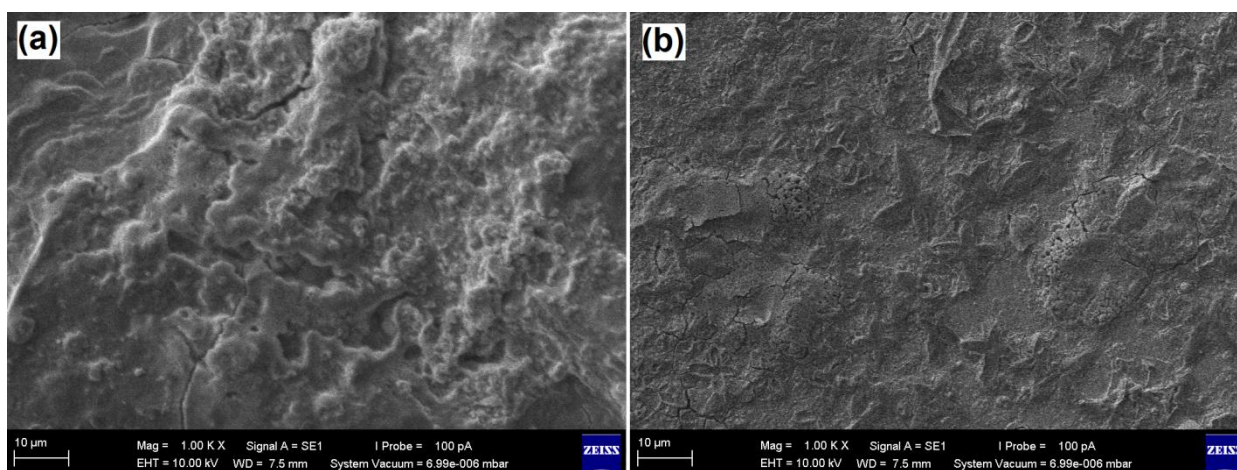


**Figure 6.** SEM micrograph of carbon steel rebar in (a) PC0 and (b) RHA10+CCA30 concrete samples after two weeks immersed in 3.5wt% NaCl solution.

#### 4. CONCLUSION

The purpose of this study was to investigate the chloride ion migration depth of cement blended with RHA and/or CCA using the EIS method. The quantitative analyses of EIS data and electrochemical parameters of the equivalent circuit model were performed on cementitious media ingress and migration depth. The SEM and compressive strength analyses were also used to investigate the depth of chloride migration in the blended cement. The results of EIS analyses showed that increasing the content of RHA and CCA decreased chloride ion migration in cementitious media, and based on the findings, EIS analyses could predict the depth of chloride ion penetration in cementitious environments with different mineral admixture replacements. Furthermore, adding 10% RHA and 30% CCA to concrete cement (RHA10+CCA30) improves resistance to chloride ion migration and corrosion while also increasing the compressive strength of concrete after four weeks of curing time. Because the synergetic effect of RHA and CCA in RHA10+CCA30 can fill in the gaps between cement particles and aggregates, SEM analyses of steel rebar incorporated into the RHA10+CCA30 sample revealed lower pitting corrosion and corrosion products compared to the control sample (PC0).

#### References

1. F.P. Bos, C. Menna, M. Pradena, E. Kreiger, W.L. da Silva, A.U. Rehman, D. Weger, R. Wolfs, Y. Zhang and L. Ferrara, *Cement and Concrete Research*, 156 (2022) 106746.
2. S. Kakooei, H.M. Akil, A. Dolati and J. Rouhi, *Construction and Building Materials*, 35 (2012) 564.
3. M. Rabi, R. Shamass and K. Cashell, *Construction and Building Materials*, 325 (2022) 126673.
4. J. Xu, W. Lan, C. Ren, X. Zhou, S. Wang and J. Yuan, *Cold Regions Science and Technology*,

- 189 (2021) 103335.
5. B.G. Basha, B.K. Rao and C.H. Rao, *Materials Today: Proceedings*, 33 (2020) 245.
  6. X. Cui, C. Li, Y. Zhang, W. Ding, Q. An, B. Liu, H.N. Li, Z. Said, S. Sharma and R. Li, *Frontiers of Mechanical Engineering*, 18 (2023) 1.
  7. C.G. Berrocal, K. Lundgren and I. Löfgren, *Cement and Concrete Research*, 80 (2016) 69.
  8. K. De Weerd, A. Colombo, L. Coppola, H. Justnes and M.R. Geiker, *Cement and Concrete Research*, 68 (2015) 196.
  9. S. Kakooei, H.M. Akil, M. Jamshidi and J. Rouhi, *Construction and Building Materials*, 27 (2012) 73.
  10. Y. Yang, M. Yang, C. Li, R. Li, Z. Said, H.M. Ali and S. Sharma, *Frontiers of Mechanical Engineering*, (2022) 1.
  11. M. Moreno, W. Morris, M. Alvarez and G. Duffó, *Corrosion Science*, 46 (2004) 2681.
  12. N. Wang, R. Zhao, L. Zhang and X. Guan, *Microporous and Mesoporous Materials*, 345 (2022) 112248.
  13. Z. Duan, C. Li, Y. Zhang, M. Yang, T. Gao, X. Liu, R. Li, Z. Said, S. Debnath and S. Sharma, *Frontiers of Mechanical Engineering*, (2022) 1.
  14. W. Xu, C. LI, Y. Zhang, H.M. Ali, S. Sharma, R. Li, M. Yang, T. Gao, M. Liu and X. Wang, *International Journal of Extreme Manufacturing*, 4 (2022) 042003.
  15. A. Jindal and G. Ransinchung, *International Journal of Pavement Research and Technology*, 11 (2018) 488.
  16. N. Jain, *Construction and Building Materials*, 27 (2012) 39.
  17. M.A. Caldarone, K.A. Gruber and R.G. Burg, *Concrete International*, 16 (1994) 37.
  18. O. Al-Amoudi, M. Maslehuddin and I.M. Asi, *Cement, Concrete and Aggregates*, 18 (1996) 71.
  19. A. Karasın and M. Doğruyol, *Advances in Materials Science and Engineering*, 2014 (2014) 1.
  20. Q. Zhang, H. Li, H. Feng and T. Jiang, *International Journal of Electrochemical Science*, 15 (2020) 6135.
  21. M.M. Johari, A. Zeyad, N.M. Bunnori and K. Ariffin, *Construction and Building Materials*, 30 (2012) 281.
  22. P. Mondal, S.P. Shah, L.D. Marks and J.J. Gaitero, *Transportation Research Record*, 2141 (2010) 6.
  23. W.Z. Shengpin Liu, *International Journal of Electrochemical Science*, 15 (2020) 3825.
  24. V. Volpi-León, L. López-León, J. Hernández-Ávila, M. Baltazar-Zamora, F. Olguín-Coca and A. López-León, *International Journal of Electrochemical Science*, 12 (2017) 22.
  25. R. Li, Z. Du, X. Qian, Y. Li, J.-C. Martinez-Camarillo, L. Jiang, M.S. Humayun, Z. Chen and Q. Zhou, *Quantitative Imaging in Medicine and Surgery*, 11 (2021) 918.
  26. T. Gao, Y. Zhang, C. Li, Y. Wang, Y. Chen, Q. An, S. Zhang, H.N. Li, H. Cao and H.M. Ali, *Frontiers of Mechanical Engineering*, 17 (2022) 1.
  27. X. Cui, C. Li, Y. Zhang, Z. Said, S. Debnath, S. Sharma, H.M. Ali, M. Yang, T. Gao and R. Li, *Journal of Manufacturing Processes*, 80 (2022) 273.
  28. X. Zhang, C. Li, Y. Zhang, D. Jia, B. Li, Y. Wang, M. Yang, Y. Hou and X. Zhang, *The International Journal of Advanced Manufacturing Technology*, 86 (2016) 3427.
  29. D.A. Adesanya and A.A. Raheem, *Construction and Building Materials*, 23 (2009) 347.
  30. D. Adesanya and A. Raheem, *Construction and Building materials*, 23 (2009) 311.
  31. O.S. Olafusi and F.A. Olutoge, *Journal of Emerging Trends in Engineering and Applied Sciences*, 3 (2012) 297.
  32. A. Gupta and A.S. Wayal, *IOSR Journal of Mechanical and Civil Engineering*, 12 (2015) 29.
  33. W. Zhang and Y. Huang, *Construction and Building Materials*, 350 (2022) 128818.
  34. R.M. Ferraro and A. Nanni, *Construction and Building Materials*, 31 (2012) 220.
  35. Z. Hu, T. Shi, M. Cen, J. Wang, X. Zhao, C. Zeng, Y. Zhou, Y. Fan, Y. Liu and Z. Zhao, *Construction and Building Materials*, 343 (2022) 128117.

36. I. Ismail, S.A. Bernal, J.L. Provis, R. San Nicolas, D.G. Brice, A.R. Kilcullen, S. Hamdan and J.S. van Deventer, *Construction and Building Materials*, 48 (2013) 1187.
37. B. Li, C. Li, Y. Zhang, Y. Wang, D. Jia and M. Yang, *Chinese Journal of Aeronautics*, 29 (2016) 1084.
38. S. Hidalgo, L. Soriano, J. Monzó, J. Payá, A. Font and M.V. Borrachero, *Applied Sciences*, 11 (2021) 773.
39. R. Li, X. Qian, C. Gong, J. Zhang, Y. Liu, B. Xu, M.S. Humayun and Q. Zhou, *IEEE Transactions on Biomedical Engineering*, (2022) 1.
40. B. Dong, Y. Wu, X. Teng, Z. Zhuang, Z. Gu, J. Zhang, F. Xing and S. Hong, *Construction and Building Materials*, 211 (2019) 261.
41. H. Li, Y. Zhang, C. Li, Z. Zhou, X. Nie, Y. Chen, H. Cao, B. Liu, N. Zhang and Z. Said, *Korean Journal of Chemical Engineering*, 39 (2022) 1107.
42. N.-u. Amin, *Journal of materials in civil engineering*, 23 (2011) 717.
43. T. Shi, Y. Liu, X. Zhao, J. Wang, Z. Zhao, D.J. Corr and S.P. Shah, *Journal of Building Engineering*, 61 (2022) 105248.
44. O. Millet, A. Mokhtar and O. Amiri, *The International Journal of Multiphysics*, 2 (2008) 129.
45. W.A. Chaparro, J.H.B. Ruiz and R.d.J.T. Gómez, *Materials Research*, 15 (2012) 57.
46. Y. Fang, H. Li, Z. Wang, K. Zhang, P. Cui and B. Dong, *IOP Conference Series: Earth and Environmental Science*, 300 (2019) 052011.
47. T. Shi, Y. Liu, Z. Hu, M. Cen, C. Zeng, J. Xu and Z. Zhao, *Materials Journal*, 119 (2022) 119.
48. H. Li, Y. Zhang, C. Li, Z. Zhou, X. Nie, Y. Chen, H. Cao, B. Liu, N. Zhang and Z. Said, *The International Journal of Advanced Manufacturing Technology*, 120 (2022) 1.
49. S. Li, B. Hu and F. Zhang, *Journal of Nanoelectronics and Optoelectronics*, 12 (2017) 1244.
50. S. Hassi, M.E. Touhami, A. Boujad and H. Benqlilou, *Construction and Building Materials*, 262 (2020) 120925.
51. X. Wang, C. Li, Y. Zhang, Z. Said, S. Debnath, S. Sharma, M. Yang and T. Gao, *The International Journal of Advanced Manufacturing Technology*, 119 (2022) 631.
52. B. Dong, Z. Gu, Q. Qiu, Y. Liu, W. Ding, F. Xing and S. Hong, *Construction and Building Materials*, 161 (2018) 577.
53. V.-w. Ramasamy, *KSCE Journal of Civil Engineering*, 16 (2012) 93.
54. G. Sua-iam, N. Makul, S. Cheng and P. Sokrai, *Construction and building materials*, 228 (2019) 116813.
55. P. Suwanmaneechot, T. Nochaiya and P. Julphunthong, *IOP Conference Series: Materials Science and Engineering*, 103 (2015) 012023.
56. Y. Yang, Y. Gong, C. Li, X. Wen and J. Sun, *Journal of Materials Processing Technology*, 291 (2021) 117023.
57. S. Ray, J. Dash, N. Devi, S. Sasmal and B. Pesala, *Terahertz, RF, Millimeter, and Submillimeter-Wave Technology and Applications VIII*, 9362 (2015) 159.
58. A. Nazari, S. Riahi, S. Riahi, S. Shamekhi and A. Khademno, *Journal of American Science* 6 (2010) 6.
59. D. Bondar, C.J. Lynsdale, N.B. Milestone, N. Hassani and A.A. Ramezaniapour, *Construction and Building Materials*, 25 (2011) 2906.
60. A. Pandey and B. Kumar, *Environmental Science and Pollution Research*, 29 (2022) 24504.
61. P. Murthi, K. Poongodi and R. Gobinath, *IOP Conference Series: Materials Science and Engineering*, 1006 (2020) 012027.